Received: 5 November 2020 | Revised: 9 December 2020 | Accepted: 19 April 2021

DOI: 10.1111/ele.13780

ECOLOGY LETTERS cnrs WILEY

PERSPECTIVE

Theory of temperature-dependent consumer–resource interactions

Alexis D. Synodinos[1] | **Bart Haegeman**[1] | **Arnaud Sentis**[2] | **José M. Montoya**[1]

[1]Theoretical and Experimental Ecology Station, CNRS, Moulis, France

[2]INRAE, Aix Marseille University, UMR RECOVER, Aix-en-Provence, France

Correspondence
Alexios D. Synodinos, Theoretical and Experimental Ecology Station, CNRS, UMR 5321, 2 Route du CNRS, Moulis 09200, France.
Email: alexios.synodinos@sete.cnrs.fr

Funding information
H2020 European Research Council, Grant/Award Number: 726176; Agence Nationale de la Recherche, Grant/Award Number: ANR-10-LABX-41

Editor: Ulrich Brose

Abstract

Changes in temperature affect consumer–resource interactions, which underpin the functioning of ecosystems. However, existing studies report contrasting predictions regarding the impacts of warming on biological rates and community dynamics. To improve prediction accuracy and comparability, we develop an approach that combines sensitivity analysis and aggregate parameters. The former determines which biological parameters impact the community most strongly. The use of aggregate parameters (i.e., maximal energetic efficiency, ρ, and interaction strength, κ), that combine multiple biological parameters, increases explanatory power and reduces the complexity of theoretical analyses. We illustrate the approach using empirically derived thermal dependence curves of biological rates and applying it to consumer–resource biomass ratio and community stability. Based on our analyses, we generate four predictions: (1) resource growth rate regulates biomass distributions at mild temperatures, (2) interaction strength alone determines the thermal boundaries of the community, (3) warming destabilises dynamics at low and mild temperatures only and (4) interactions strength must decrease faster than maximal energetic efficiency for warming to stabilise dynamics. We argue for the potential benefits of directly working with the aggregate parameters to increase the accuracy of predictions on warming impacts on food webs and promote cross-system comparisons.

KEYWORDS
biomass distributions, climate change, community stability, consumer, food webs, interaction strength, resource dynamics, temperature dependence

INTRODUCTION

Temperature strongly regulates consumer–resource interactions that constitute the fundamental blocks of ecosystems (Amarasekare, 2019; Montoya & Raffaelli, 2010; O'Connor et al., 2009; Petchey et al., 2010; Rall et al., 2012), and anthropogenic climate change will, in most cases, increase mean temperatures (IPCC, 2013). Therefore, understanding and predicting the impacts of warming on consumer–resource interactions has attracted much interest (Binzer et al., 2012; Thakur et al., 2017; Vasseur & McCann, 2005). A breakthrough occurred with the postulation that metabolic rate increases exponentially with temperature, with the slope (activation energy) conserved across levels of organisation (Brown et al., 2004; Gilooly et al., 2001). However, activation energies can vary significantly amongst organisms and biological rates (Dell et al., 2011; Réveillon et al., 2019). In addition, the thermal response curve of biological rates can decrease at high temperatures, producing a unimodal thermal dependence shape (Deutsch et al., 2008; Englund et al., 2011; Pörtner & Farrell, 2008; Uiterwaal & DeLong, 2020). This lack of consensus regarding the exact shape of the temperature dependence of physiological rates (e.g., ingestion rates), behavioural traits (e.g., consumer search or attack rates) or production (carrying capacity) has contributed to diverging, sometimes contradicting, predictions of how consumer–resource interactions will respond to warming (e.g., Sentis et al., 2012; Vucic-Pestic et al., 2011).

 © 2021 John Wiley & Sons Ltd.

A DUAL APPROACH TO ADDRESS THE DIVERGENCE IN PREDICTIONS

Even though biomass distributions and stability have been much studied properties of consumer–resource communities and food webs (Barbier & Loreau, 2019; Bideault et al., 2020; Rall et al., 2010, 2012; Uszko et al., 2017), their predicted responses to warming vary. Biomass ratios have been theorised to increase (Gilbert et al., 2014; Rip & McCann, 2011) or decrease (Vasseur & McCann, 2005) monotonically with warming, though experimentally derived data have mainly yield unimodal responses (Fussmann et al., 2014; Uszko et al., 2017). Likewise, the effects of warming on stability remain unclear. Using data on specific rates (e.g., consumer ingestion and metabolism), studies have inferred that stability either increases monotonically (Fussmann et al., 2014; Rall et al., 2010, 2012; Vucic-Pestic et al., 2011) or responds unimodally (Betini et al., 2019; Sentis et al., 2012) to warming. Theoretical work on stability, in particular the onset of oscillations, expands decades (May, 1972; Rosenzweig & MacArthur, 1963). Vasseur and McCann (2005) showed that warming will destabilise consumer–resource communities when the consumer metabolic rate increases slower than the ingestion rate. Johnson and Amarasekare (2015) demonstrated the pivotal role of the temperature dependence of carrying capacity—rather than metabolism and ingestion—in determining warming–stability relationships. All these examples demonstrate that the mixed predictions, whether empirically derived or theoretical, originate from two distinct sources: the different parameters hypothesised to be driving community responses and the thermal dependence shapes of these parameters. To improve the accuracy of predictions regarding the effects of warming on consumer–resource communities, we need to establish which biological parameters drive community properties (biomass distribution and stability) and to acquire a mechanistic understanding of how their thermal dependence shapes affect community properties.

A dual approach utilising sensitivity analysis and the application of aggregate parameters can address both these issues (Figure 1). In this study, we illustrate this dual approach using the popular Rosenzweig–MacArthur model (Rosenzweig & MacArthur, 1963), although the combined approach of a sensitivity analysis and parameter aggregation is not restricted to this model.

The dual approach benefits from tackling the problem of mixed predictions from different angles. On the one hand, sensitivity analysis establishes the parameters that most strongly influence the community property of interest: it quantifies the increase in a response variable with respect to a small increase in a parameter. It has been extensively used in population ecology and demography (Caswell, 2019), with implications for applied ecology (Manlik et al., 2018). Since the relative importance of parameters can change along the temperature gradient, a sensitivity analysis allows us to determine the temperatures at which changes in the values of different parameters have the strongest relative impact (Zhao et al., 2020).

On the other hand, we can aggregate groups of the primary parameters into fewer, biologically meaningful and empirically measurable quantities. The use of such aggregate parameters reduces the complexity of theoretical analyses, provides a mechanistic interpretation for the difference in predictions and facilitates the comparison amongst predictions (Barbier & Loreau, 2019; Bideault et al., 2020). Experimentally, replacing multiple measurements of individual parameters with measurements of the aggregates could also restrict the room for divergent findings. The seminal work of Yodzis and Innes (1992) reduced the analysis of consumer–resource interactions to two aggregate parameters; consumer maximal energetic efficiency and a measure of resource abundance. A variation of maximal energetic efficiency (termed energetic efficiency) has been widely used in empirical studies. However, rather than being measured directly, energetic efficiency has been derived from measurements of its principle components, that is, feeding and metabolic rates (Rall et al., 2010; Sentis et al., 2012; Vucic-Pestic et al., 2011). Gilbert et al., (2014) posited that interaction strength alone—defined as the impact of the consumer on the resource population density—could capture the effects of warming on the stability of consumer–resource interactions. However, their approach was based on a type I (nonsaturating) functional response, whereas most consumer–resource species pairs typically produce type II or III (saturating) functional responses (Jeschke et al., 2004). Moreover, the thermal dependence of interaction strength did not match the impact of warming on stability for type II or III functional responses (Uszko et al., 2017), pointing to a more complex relationship between interaction strength, warming and stability. We use two aggregate parameters which govern dynamics in the Rosenzweig–MacArthur model: the maximal energetic efficiency of the consumer population, defined as the ratio of energetic gains through ingestion with no resource limitation (i.e., maximal energetic gains) over energetic losses associated to metabolic demand (Yodzis & Innes, 1992) and interaction strength, measured as the ratio of resource population density without consumers to resource population density with consumers (Gilbert et al., 2014).

Thus, our dual approach identifies the parameters causing the divergence in predictions through the sensitivity analysis and simplifies complex theoretical explorations and empirical measurements through the two aggregate parameters (Figure 1). The combination of sensitivity analysis and parameter aggregation can be generally applied as it is not tailored to a specific model of consumer–resource interactions; sensitivity analysis (e.g., Chitnis et al., 2008) and parameter aggregation (e.g., Barbier & Loreau, 2019) have been used

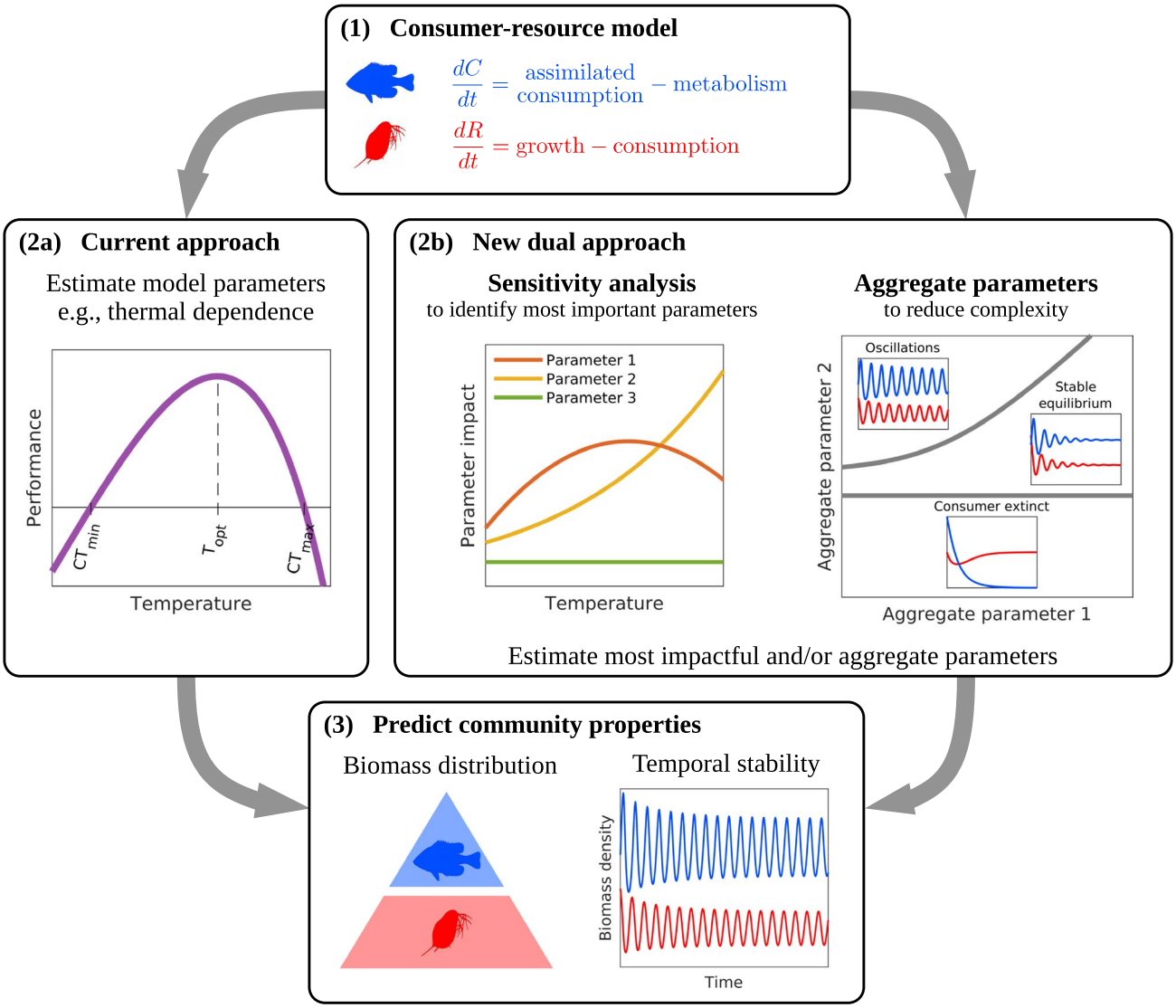


FIGURE 1 Illustration of the current and new dual approaches to predict the impact of global change drivers on community properties. (1) Predictions require a consumer–resource model; the Rosenzweig–MacArthur model (Rosenzweig & MacArthur, 1963) or its bioenergetic equivalent (Yodzis & Innes, 1992) have been used most commonly for ectotherm consumer–resource pairs. (2a) The current approach is to experimentally measure the response of parameters along an environmental gradient, for example, the thermal dependence of the resource population maximal growth rate with critical temperatures, CT_{min}, CT_{max}, and the thermal optimum, T_{opt}. These measurements are used to parameterise the model. Importantly, not all parameters are measured but rather those which are considered significant (e.g., consumer feeding and metabolic rates for warming–stability relationships). Assuming the remaining parameter values, the model is then used to generate predictions. (2b) Our new dual approach aims to increase the accuracy of predictions and facilitate their comparison. First, a sensitivity analysis determines which parameters have the greatest relative impact on the community property of interest along the environmental gradient. Then, aggregate parameters which represent biologically measurable quantities are used to express all sensitivities and determine the dynamics. Collapsing analyses to the two aggregate parameters reduces complexity and increases mechanistic tractability. This facilitates the choice of which parameters need to be measured. (3) Through the empirical determination of the most appropriate parameters (either from the original model parameters or the aggregate parameters themselves) and the reduction in the number of measurements required, prediction accuracy improves. The advantages of the new dual approach are twofold. First, as the sensitivity analysis will have identified the most impactful parameters, the source of divergence in predictions can be isolated. Second, the aggregates represent standardised measurable population-level indicators across systems, making theoretical or empirical predictions directly comparable

independently for different models. Here, we apply this to the Rosenzweig–MacArthur model (Rosenzweig & MacArthur, 1963), a model frequently used to study the effects of temperature on consumer–resource interactions (Daugaard et al., 2019; Dee et al., 2020; Fussmann et al., 2014; Uszko et al., 2017). We focus on consumer–resource biomass ratio and a stability metric quantifying the proximity to oscillations; these two variables dominate the literature on the effects of warming on consumer–resource communities (Betini et al., 2019; Rall et al., 2008; Uszko et al., 2017; Vasseur & McCann, 2005). We implement different thermal parameterisations from the literature to elucidate how the relative importance of different parameters and their

varying thermal dependence shapes impact predicted effects of temperature on consumer–resource interactions. Based on our results, we make four predictions that can be theoretically and empirically tested.

THE DUAL APPROACH

In this study we illustrate the application of the dual approach (i.e., parameter sensitivity and aggregation) using the Rosenzweig–MacArthur model with a type II functional response (Rosenzweig & MacArthur, 1963). This model describes the rate of change in resource and consumer biomass densities:

$$\frac{dR}{dt} = r\left(1 - \frac{R}{K}\right)R - \frac{aR}{1 + ahR}C, \tag{1}$$

$$\frac{dC}{dt} = \left(e\frac{aR}{1 + ahR} - m\right)C, \tag{2}$$

R and C are the resource and consumer species biomass densities, respectively. Resource growth is logistic, with an intrinsic growth rate, r, and carrying capacity, K. Resource biomass density is limited by the consumer through a saturating Holling type II functional response with attack rate, a and handling time, h. Consumer growth is proportional to the assimilated consumed biomass, with e the dimensionless assimilation efficiency; losses occur due to metabolic costs, m. Below, we present the formulas most relevant to our study; an extensive analysis of the model is available in Supporting Information S1. We chose a type II response due to its prevalence in many natural consumer–resource interactions (Jeschke et al., 2004), though our approach works for the general form of the functional response (Supporting Information S2). Additionally, the functional response can be defined with respect to attack rate and handing time, $f(R) = \frac{aR}{1+ahR}$, or maximum consumption rate, J, and half-saturation density, R_0, $f(R) = \frac{JR}{R_0 + I}$ (Supporting Information S3).

Stability and aggregate parameters

The Rosenzweig–MacArthur model produces population cycles (oscillations) with increasing energy fluxes (Rip & McCann, 2011). Therefore, the coexistence equilibrium can be stable or unstable, where dynamics oscillate around the unstable equilibrium (i.e., a limit cycle). The switch from stable to unstable dynamics occurs at a Hopf bifurcation. Theoretical studies have analysed this qualitative change (Amarasekare, 2015; Vasseur & McCann, 2005; Yodzis & Innes, 1992) because these distinct stability regimes translate to different temporal dynamics, with oscillations leading to greater variability over time. We applied a stability metric that quantifies the tendency of the dynamics to oscillate (Johnson & Amarasekare, 2015).

We assumed that dynamics had converged to the stable equilibrium or the limit cycle and determined the coexistence equilibria analytically (Supporting Information S1). In the latter case, we retrieved the unstable equilibrium which is approximately equal to the time-averaged biomass values along the limit cycle. From the equilibria values, we get the biomass ratio:

$$\mathcal{B} = \frac{C_S}{R_S} = er\frac{aK(e - mh) - m}{amK(e - mh)}. \tag{3}$$

We observed certain repeated parameter groupings (i.e., aggregate parameters) that governed the dynamics (Supporting Information S1). Such aggregates have been previously used for the analysis of the Rosenzweig–MacArthur model (Vasseur & McCann, 2005; Yodzis & Innes, 1992). The aggregates we selected represent ecological mechanisms which can be empirically measured. These are maximal energetic efficiency, $\rho = \frac{e}{mh}$, and interaction strength, $\kappa = ahK\left(\frac{e}{mh} - 1\right)$. A closer look at ρ and κ elucidates their biological meaning. $\frac{1}{h}$ is the saturation value of the functional response and thus represents the maximum consumption rate, J. Hence, ρ can be written as follows:

$$\rho = \underbrace{e}_{\text{consumer assimilation efficiecny}} \times \underbrace{J}_{\text{maximum consumption rate}} \times \underbrace{\frac{1}{m}}_{\text{consumer metabolic loss}} = \frac{\text{maximal energetic gain}}{\text{energetic loss}},$$

ρ quantifies the energetic gain-to-loss ratio of the consumer population biomass assuming its maximum feeding rate is realised (i.e., unlimited resources). ρ was introduced by Yodzis and Innes (1992) as a key aggregate parameter to understand food web dynamics. In empirical studies, a variant of ρ termed energetic efficiency, y, has been often applied (Rall et al., 2010; Sentis et al., 2012, 2017). Unlike ρ, y is a function of the full functional response term and hence also depends on resource density, $y = \frac{e \times f(R)}{m}$, where $f(R) = \frac{aR}{1+ahR}$ at a specified resource density, R.

The second aggregate parameter, κ, can be rewritten in terms of the resource population density:

$$\kappa = ahK\left(\frac{e}{mh} - 1\right) = \frac{K}{R_S},$$

κ is the ratio of the resource equilibrium density without consumers (carrying capacity) to the resource equilibrium density with consumers. κ quantifies the effect

of the consumer population on the resource population and measures interaction strength (Berlow et al., 1999; Gilbert et al., 2014).

Using ρ and κ, we determine the conditions for positive resource (Equation 4) and consumer (Equation 5) densities, as well as the Hopf bifurcation (Equation 6) (Supporting Information S1):

$$\rho > 1, \tag{4}$$

$$\kappa > 1, \tag{5}$$

$$\kappa - \rho - 1 = 0, \tag{6}$$

$\kappa > 1$ requires that $\rho > 1$ (Supporting Information S1). Hence, $\kappa > 1$ defines the consumer feasibility boundary. We do not consider stochastic extinctions which may occur due to large-amplitude oscillations when population biomass reaches very low values.

To determine stability, we adjusted the metric of Johnson and Amarasekare (2015) so that it vanished at the Hopf bifurcation (Supporting Information S4). This metric, $\mathcal{S}$, defines stability solely in relation to the Hopf bifurcation.

$$\mathcal{S} = -\frac{(\kappa - \rho - 1)}{\rho - 1},$$

$\mathcal{S} > 0$ corresponds to a stable equilibrium and $\mathcal{S} < 0$ to oscillations.

Sensitivity analysis

We performed a sensitivity analysis of the biomass ratio ($\mathcal{B}$) and the stability metric ($\mathcal{S}$) with respect to the original model parameters (i.e., r, a, h, e and m). A sensitivity analysis quantifies the effect of a small change in a parameter on the response variable. Typically, while one parameter is being perturbed, all others are assumed to remain constant and correlations between the parameters are not explicitly considered. Nevertheless, this approach can be applied in cases of correlated parameter change without a loss of accuracy (Supporting Information S5, 5.1.1). As we demonstrate analytically (Supporting Information S5, 5.1.1, equation S5.3), if environmental conditions (e.g., temperature) induce correlated changes in the parameters, the sensitivity of the response variable (e.g., $\mathcal{B}$ or $\mathcal{S}$) with respect to the environmental conditions can be reconstructed by a linear combination of the sensitivities of the response variables to the individual parameters weighted by the parameter sensitivity to environmental conditions (Supporting Information S5, 5.1.1, Figure S5.1). Thus, even though our approach does not explicitly consider parameter correlations, it contains all the necessary information to account for such covariance. We illustrate this numerically by reproducing the sensitivity of the stability metric ($\mathcal{S}$) with respect to temperature through the linear combination of the weighted sensitivity of stability with respect to the individual parameters. We do this for two parameter sets (Fussmann et al., 2014; Uszko et al., 2017) for which parameters are strongly correlated (Supporting Information S5, 5.1.1, Table S4, Figure S5.2). Different types of sensitivity indices exist such as simple sensitivity and elasticity (Caswell, 2019; Manlik et al., 2018). Here we used elasticity for biomass ratio ($\mathcal{B}$) and an adjusted elasticity for stability ($\mathcal{S}$) (Supporting Information S5, 5.1.2), both dimensionless to facilitate direct comparisons between parameter sensitivities.

Elasticity is a proportional sensitivity, quantifying how a relative change in a parameter translates into a relative change in the variable, otherwise known as the log-scaled sensitivity (Manlik et al., 2018). Thus, the elasticity of $\mathcal{B}$ with respect to parameter x is given by the following:

$$\partial_x \mathcal{B} = \frac{\frac{\partial \mathcal{B}}{\mathcal{B}}}{\frac{\partial x}{x}} = \frac{\partial \ln(\mathcal{B})}{\partial \ln(x)}.$$

If $\partial_x \mathcal{B} = 1$, a relative increase of 10% in parameter x causes a relative increase of 10% in variable $\mathcal{B}$. Conversely, $\partial_x \mathcal{B} = -1$ implies that a relative increase of 10% in parameter x results in relative decrease of 10% in $\mathcal{B}$.

For the sensitivity of the stability metric, $\mathcal{S}$, we used a variation of the elasticity. We defined the sensitivity of $\mathcal{S}$ as the incremental change in $\mathcal{S}$ induced by a relative change in parameter x. Our adjustment was possible due to $\mathcal{S}$ being dimensionless, and it prevents sensitivities from diverging to infinity close to the Hopf bifurcation without altering the outcome of our analysis (Supporting Information S5, 5.1.2).

$$\partial_x \mathcal{S} = \frac{\partial \mathcal{S}}{\frac{\partial x}{x}} = \frac{\partial \mathcal{S}}{\partial \ln(x)},$$

$\partial_x \mathcal{S} = 1$ means that a relative increase in parameter x of 10% causes an absolute increase of 0.1 in $\mathcal{S}$ and has a stabilising effect. If $\partial_x \mathcal{S} = -1$, the same relative increase in x leads to decrease of 0.1 in $\mathcal{S}$ with a destabilising effect.

The magnitude and sign of each sensitivity determine how strongly and in what direction (increasing or decreasing the response variable) the parameter perturbation impacts the variable, respectively. We used the magnitudes to rank the relative importance of all parameters.

All sensitivities could be expressed in terms of ρ and κ. Hence, in a plane with ρ and κ as axes, sensitivities are fully determined and can be ranked by magnitude, splitting the parameter space into regions where different parameters have the highest, second highest, and so forth and sensitivity. Here, we present figures where

the regions are determined by the top two ranked sensitivities; we do not portray changes in the rankings of the lowest sensitivities (see Figures S5.5 and S5.6 for the complete regions). The biomass ratio and stability metric have different sensitivity expressions and, therefore, produced different regions. For each variable, the regions remain fixed irrespective of the parameterisation used, because the sensitivity expressions stem from the model equations. The ρ–κ plane provides additional information, such as the feasibility boundary (Equation 5) and the position of the Hopf bifurcation (Equation 6).

Temperature parameterisations

To demonstrate the impacts of different parameter thermal dependencies, we implemented temperature parameterisations from the literature. Maintenance respiration rate, m, typically increases exponentially with temperature (Brown et al., 2004) following the Arrhenius equation (Sentis et al., 2017; Uszko et al., 2017; Vasseur & McCann, 2005). However, the thermal dependencies of resource growth rate, r, attack rate, a, and handling time, h, have been represented either through the Arrhenius equation (Binzer et al., 2016; Vasseur & McCann, 2005) or as unimodal functions (Amarasekare, 2015; Uiterwaal & DeLong, 2020; Uszko et al., 2017; Zhang et al., 2017; Zhao et al., 2020). Carrying capacity, K, and consumer assimilation efficiency, e, have a less clear connection to temperature (Dee et al., 2020; Uszko et al., 2017). We selected two parameterisations related to the ongoing debate surrounding the importance of including the decreasing part of the biological rates beyond the optimal temperature (Pawar et al., 2016) and used these as an illustrative comparison. The 'unimodal' model had a unimodal parameterisation for r, a (both hump-shaped) and h (U-shaped), the Arrhenius equation for m (increasing) and constant K and e (Uszko et al., 2017). We compared this to a 'monotonic' parameterisation where all thermal dependencies (r, a, m increasing; h, K decreasing) follow the Arrhenius equation and e is constant (Fussmann et al., 2014). Following this comparison, we plotted four additional parameterisations from the literature onto the ρ–κ plane to broaden the comparison and demonstrate the simplicity of applying the approach to empirically derived measurements. These consisted of two similar monotonic parameterisations (Binzer et al., 2016; Vucic-Pestic et al., 2011), one where only a was hump-shaped (Sentis et al., 2012) and one which though monotonic, included some distinctive thermal dependencies—exponentially increasing $K(T)$ and $e(T)$ and constant h (Archer et al., 2019). We provide a description of the studies and details of their parameterisations in Supporting Information S6.

We should note that not all parameterisations included the resource growth rate, r, so the biomass ratio could not be calculated in these cases. However, we could calculate ρ and κ and, hence, the biomass ratio elasticities for all parameterisations. Thus, we could determine how biomass ratio sensitivities to individual parameters changed with warming regardless of the actual biomass ratio values. By including studies which had not measured resource growth or estimated the biomass ratio, we broadened the scope of the comparison of the biomass ratio sensitivities. Though this does not represent an exhaustive list of parameterisations, we were restricted to parameterisations which could be used to parameterise the Rosenzweig–MacArthur model with a type II response and whose available parameters could yield ρ and κ. 'Mild' and 'extreme' temperatures, as well as 'close' or 'far' from consumer extinction, are defined relative to each parameterisation's temperature range and feasibility boundaries, respectively. The feasible temperature range was determined by interaction strength ($\kappa > 1$) with the temperature extremes corresponding to the point of consumer extinction. This condition assumes that resources have a broader thermal range than consumers (e.g., Rose & Caron, 2007; West & Post, 2016). If resources go extinct at temperatures consumers could withstand, then the feasibility boundary becomes dependent on resource growth rate, r (Amarasekare, 2015). The parameterisations we present come from ectotherms, where environmental temperatures correspond to the organisms' temperatures. However, our approach can be transferred to endotherms as it does not depend on a specific thermal parameterisation.

SENSITIVITIES DEPEND ON PROXIMITY TO THERMAL BOUNDARIES

Biomass ratio: Always most sensitive to e and m

We analytically obtained four groups of biomass ratio elasticity magnitudes, $\partial_e \mathcal{B} = |\partial_m \mathcal{B}|$, $\partial_K \mathcal{B} = \partial_a \mathcal{B}$, $\partial_r \mathcal{B}$ and $\partial_h \mathcal{B}$ (Table 1). e and m always have the largest elasticity

TABLE 1 Sensitivities of the biomass ratio ($\partial_x \mathcal{B}$) and of the stability metric ($\partial_x \mathcal{S}$) with respect to the six original model parameters

Parameter	Consumer–resource biomass ratio, $\mathcal{B}$	Stability metric, $\mathcal{S}$
X	$\partial_x \mathcal{B} = \frac{\partial \ln(\mathcal{B})}{\partial \ln(x)}$	$\partial_x \mathcal{S} = \frac{\partial \mathcal{S}}{\partial \ln(x)}$
r	1	0
K	$\frac{1}{\kappa - 1}$	$-\frac{\kappa}{\rho - 1}$
a	$\frac{1}{\kappa - 1}$	$-\frac{\kappa}{\rho - 1}$
h	$-\frac{1}{(\rho - 1)(\kappa - 1)}$	$\frac{\kappa(1-\rho)+2\rho}{(\rho-1)^2}$
e	$\frac{\rho}{(\rho - 1)(\kappa - 1)} + 1$	$-\frac{2\rho}{(\rho-1)^2}$
m	$-\frac{\rho}{(\rho - 1)(\kappa - 1)} - 1$	$\frac{2\rho}{(\rho-1)^2}$

Note: All sensitivities are expressed in terms of ρ and κ.

and hence the strongest relative impact on the biomass ratio ($\partial_e B = |\partial_m B| > \partial_K B, \partial_a B, \partial_r B, |\partial_h B|$). Increasing e increases the biomass ratio ($\partial_e B > 0$); increasing m reduces it ($\partial_m B < 0$). K and a have equal and positive elasticities ($\partial_K B = \partial_a B > 0$), both increasing the biomass ratio. The elasticity of r is constant, $\partial_r B = 1$, a directly proportional positive effect on B. Increasing h reduces the biomass ratio, $\partial_h B < 0$. These are general results, independent of any model parameterisation (with temperature or otherwise) following directly from the Rosenzweig–MacArthur model's equations.

Biomass ratio: High r elasticity far from thermal boundaries

Both the 'unimodal' and 'monotonic' temperature parameterisations produced a unimodal biomass ratio thermal dependence (Figure 2). The unimodal parameterisation induced thermal boundaries to the community at both low (1°C) and high (33°C) temperatures (Figure 2a). The biomass ratio exceeded 1 for most temperatures (higher consumer than resource biomass), peaked at 14°C around $B \approx 5.5$ and decreased rapidly to 0 as it approached both thermal boundaries (low and high temperature extremes). The biomass ratio of the monotonic parameterisation (Figure 2b) increased with warming from low temperatures and peaked at $B \approx 0.19$, before decreasing to 0 at high temperatures (27.5°C). The two parameterisations are derived from different systems, hence the different temperature ranges.

In both parameterisations, sensitivity to e and m was highest throughout (Figure 2c,d)—as expected from the analytical findings. Elasticities were split into two groups at mild temperatures: e, m and r had the highest elasticity with $\partial_e B = |\partial_m B| \approx \partial_r B = 1$, while a, h and K elasticities were very low. Approaching the temperature extremes all elasticities besides $\partial_r B$ diverged; $\partial_h B$ diverged faster than $\partial_K B = \partial_a B$ in the unimodal parameterisation (Figure 2c), while the opposite occurred in the monotonic one (Figure 2d).

Expressing the elasticities in terms of ρ and κ (Table 1) reduces the sensitivity analysis to two dimensions. Ranking the elasticity magnitudes creates distinct regions in the ρ–κ plane which correspond to different elasticity ranking orderings and provide a mechanistic overview of which elasticities dominate where (Figure 3a). e and m always have the highest elasticity, so the three regions reflect changes in the second highest-ranked elasticity. Regions adjacent to consumer extinction ($\kappa = 1$) have high sensitivity to either h (red region) or to a and K (yellow region). r elasticity is highest in

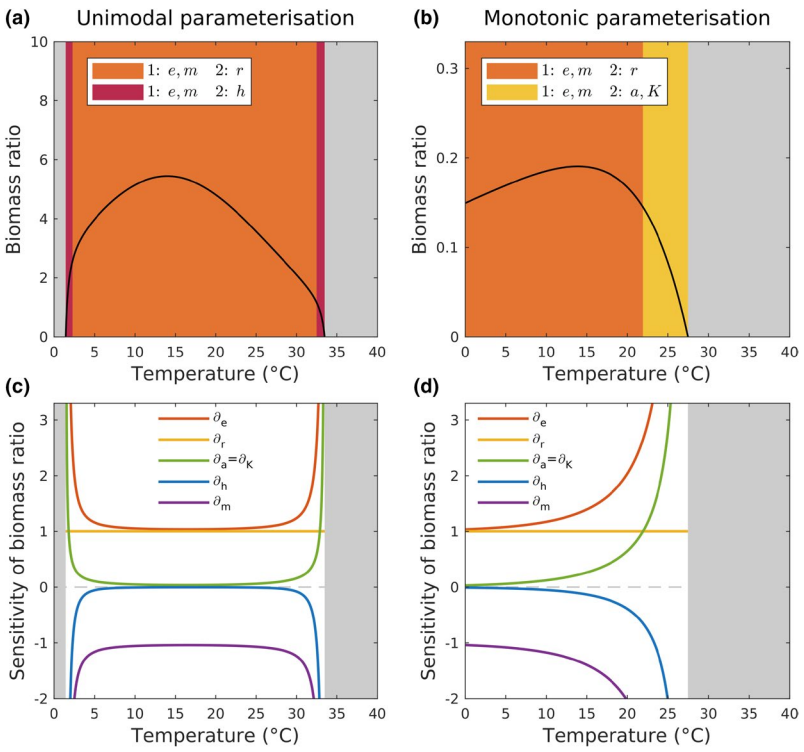


FIGURE 2 Consumer–resource biomass ratios for the (a) unimodal and (b) monotonic parameterisations along the temperature gradient. Feasible temperature ranges are constrained by the condition of positive biomass densities for both consumer and resource (grey areas correspond to consumer extinction). The different background colours correspond to different elasticity rankings of model parameters (see legend). Panels (c) and (d) provide the values of the six parameter elasticities along the temperature gradient for the unimodal and monotonic parameterisations, respectively

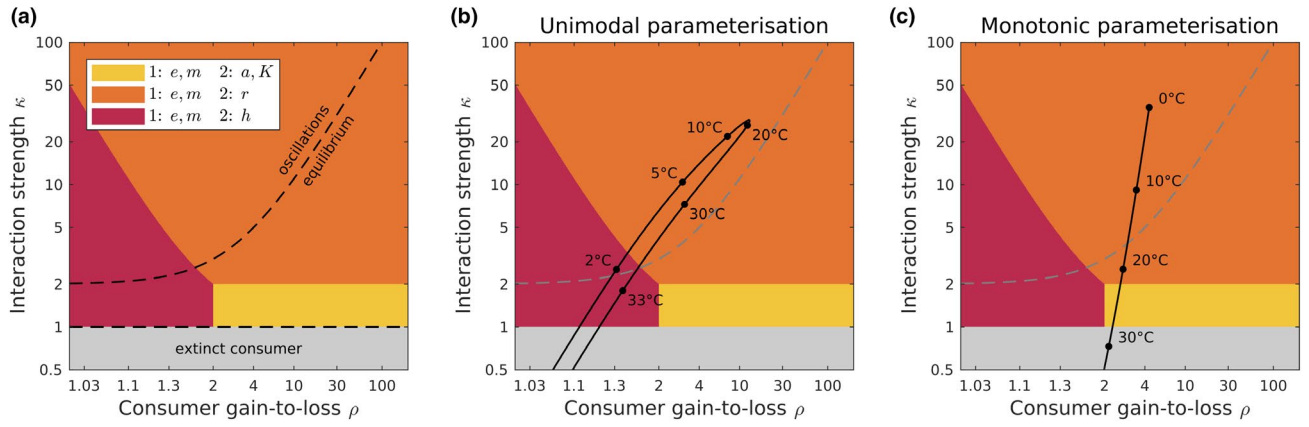


FIGURE 3 3(a) Biomass ratio elasticity rankings in the ρ–κ plane. The plane is split into regions (different colours) which correspond to different parameters having the top-two largest elasticities. These regions have been derived from the analytic expressions of the elasticities (Table 1). e and m elasticities always rank first. Close to consumer extinction h, ranks second highest at low ρ ($\rho < 2$, red region) and a and K at higher ρ ($\rho > 2$, yellow region). r ranks second highest far from consumer extinction (orange region). The plane includes the feasibility boundary ($\kappa = 1$) and the Hopf bifurcation (dotted curve splitting the plane into stable equilibrium and oscillations). For the (b) unimodal and (c) monotonic parameterisations from the literature, the thermal dependencies of $\rho = \frac{e}{mh}$ and $\kappa = \frac{K}{R_S}$ were calculated. This yielded a trajectory for each parameterisation (solid black line). The paths of the trajectories demonstrate the elasticity of the biomass ratio along the temperature gradient for each parameterisation

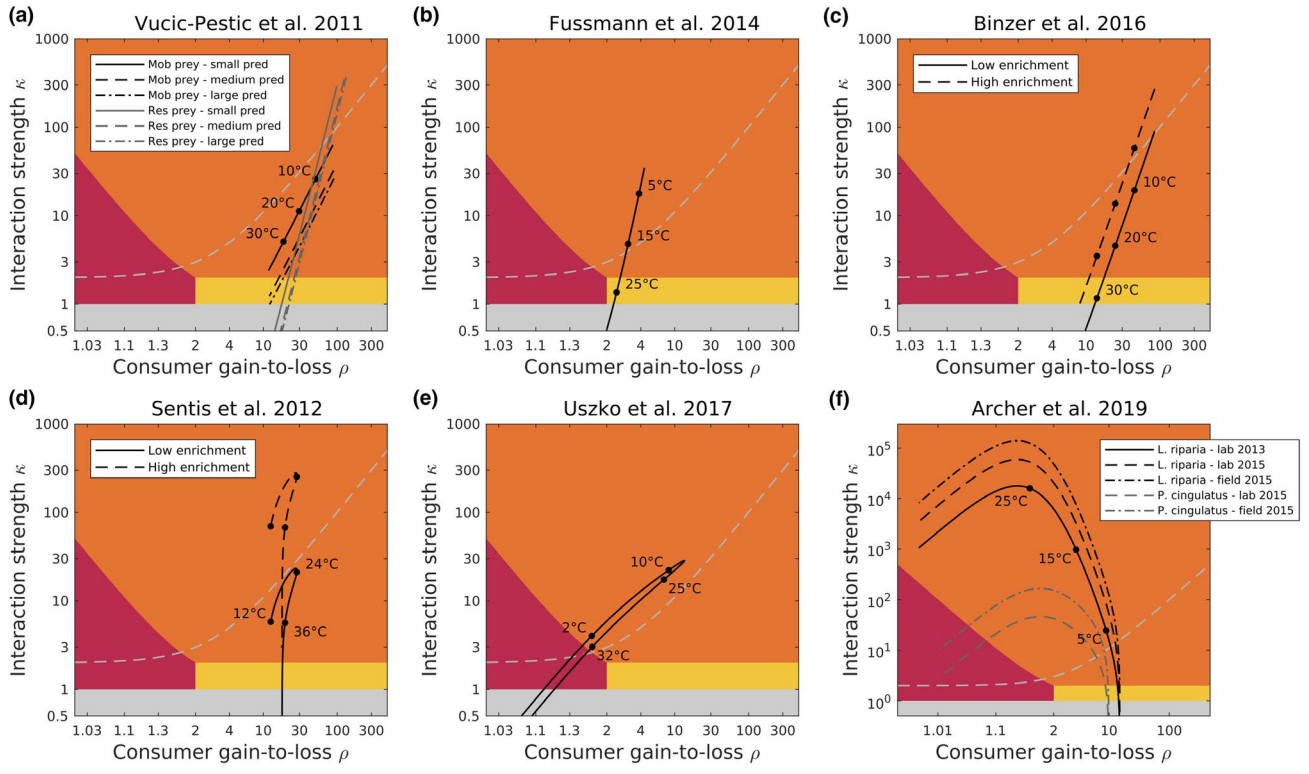


FIGURE 4 Trajectories of the six empirical temperature parameterisations in the ρ–κ plane: (a) Vucic-Pestic et al., (2011) with six different experiments—three predator size classes and two types of prey, (b) Fussmann et al., (2014), (c) Binzer et al., (2016) with two levels of enrichment, (d) Sentis et al., (2012), with two levels of enrichment, (e) Uszko et al., (2017), (f) Archer et al., (2019) with two prey types and three measurements. Panels (a–c) have monotonic thermal dependences for a, m (increasing) and h, K (decreasing) and a constant e. Panel (d) has a unimodal thermal performance curve for a (hump-shaped), constant e and K, monotonic h (decreasing) and m (increasing). Panel (e) has a unimodal (U-shaped) h and a (hump-shaped) thermal dependence, constant e and monotonic K, m (increasing). Panel (f) has monotonic a, K, m, e (increasing) and h constant. All parameter values are detailed in Supporting Information S6. The coloured regions demonstrate the different biomass ratio sensitivity rankings (see legend in Figure 3a). The trajectories (solid black lines) for each parameterisation are derived from calculating the thermal dependence of $\rho = \frac{e}{mh}$ and $\kappa = \frac{K}{R_S}$ (see *Temperature dependencies and parameterisations* for details)

the region farthest from consumer extinction (orange region). The two temperature parameterisations were mapped onto this plane by calculating their ρ and κ values (Figure 3b,c). Despite the two trajectories being markedly different, both occupied the region where r ranked second highest for most temperatures. The unimodal parameterisation produced a unimodal trajectory, crossing the consumer extinction threshold at low and high temperatures (Figure 3b). The monotonic parameterisation's trajectory converged monotonically towards consumer extinction with increasing temperature (Figure 3c).

All other parameterisations from the literature also occupied the region of high r elasticity for most temperatures, far from their thermal boundaries (Figure 4). The three similar monotonic parameterisations produced monotonic trajectories (Figure 4a–c) which started in the region of high r elasticity and converged monotonically towards consumer extinction ($\kappa = 1$). With a hump-shaped thermal dependence of attack rate, a unimodal trajectory emerged (Figure 4d). At low temperatures, it occupied the region of high r elasticity but moved away from consumer extinction. With further warming, the trajectory switched direction and followed the same path as the monotonic parameterisations, crossing the consumer extinction boundary. A unimodal thermal dependence for attack rate (hump-shaped) and handling time (U-shaped) (Figure 4e), induced extinctions at low and high temperatures imposing a unimodal trajectory. Unlike all previous parameterisations, the trajectory crossed the extinction threshold in the region of high h elasticity. The final parameterisation, though monotonic, yielded unimodal trajectories (Figure 4f). A monotonically increasing $K(T)$ (as opposed to decreasing in the other monotonic parameterisations and constant in the unimodal ones) initially forced the trajectory away from consumer extinction, albeit within the region of high r elasticity. Consumer energetic efficiency ρ decreased, pushing consumers towards extinction, thus forcing an abrupt decline towards the consumer boundary.

Stability most sensitive either to e and m or to a and K

Similarly to the biomass ratio, the analytical approach for the stability sensitivities yielded results conserved independently of the temperature parameterisations (Table 1): equal sensitivity magnitudes pairwise for e and m and for a and K (i.e., $|\partial_e \mathcal{S}| = \partial_m \mathcal{S}$ and $|\partial_K \mathcal{S}| = |\partial_a \mathcal{S}|$), negative stability sensitivities of e, a and K ($\partial_e \mathcal{S}$, $\partial_a \mathcal{S}$, $\partial_K \mathcal{S} < 0$) implying that they destabilise dynamics, a positive sensitivity of m ($\partial_m \mathcal{S} > 0$) indicating a stabilising effect. h can be either stabilising or destabilising, and r does not affect the stability regime ($\partial_r \mathcal{S} = 0$).

The unimodal temperature parameterisation exhibited oscillations ($\mathcal{S} < 0$) over most temperatures (Figure 5a). Only at low and high thermal extremes did dynamics briefly stabilise prior to consumer extinction.

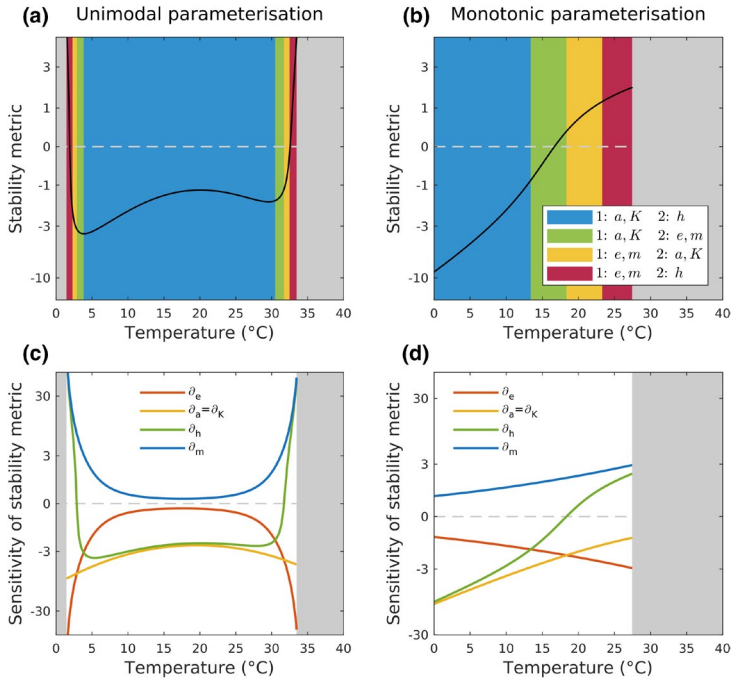


FIGURE 5 The thermal dependence of the stability metric, $\mathcal{S}$, for the (a) unimodal and (b) monotonic parameterisations. $\mathcal{S} > 0$ corresponds to stable dynamics, $\mathcal{S} < 0$ to oscillations. $\mathcal{S} = 0$ (dotted line) corresponds to the Hopf bifurcation. The coloured temperature ranges highlight regions of different sensitivity rankings. For temperatures beyond the community feasibility boundaries, the areas are greyed out. In (c) and (d), the sensitivity to each parameter is plotted along the temperature gradient for the unimodal and monotonic parameterisations, respectively. As resource growth rate does not affect stability (Table 1), we do not plot $\partial_r \mathcal{S} = 0$

The monotonic temperature parameterisation produced oscillations at low temperatures ($\mathcal{S} < 0$), crossed a Hopf bifurcation at 17°C and dynamics were stable ($\mathcal{S} > 0$) thereafter (Figure 5b). In both cases, stability close to consumer extinction was most sensitive to consumer assimilation efficiency, e, and metabolism, m, ($|\partial_e \mathcal{S}| = \partial_m \mathcal{S}$) followed by handling time, h (Figure 5c,d). Moving away from the thermal boundaries, attack rate, a, and carrying capacity, K, increased in relative importance. Furthest away from the thermal boundaries, stability was most sensitive to changes a and K, followed by h. Even though $\partial_h \mathcal{S}$ did not rank highest in any temperature range, it was a close second at the temperature extremes (second to $|\partial_e \mathcal{S}| = \partial_m \mathcal{S}$) or furthest away from them (second to $|\partial_K \mathcal{S}| = |\partial_a \mathcal{S}|$). Additionally, h switched from destabilising at mild temperatures ($\partial_h \mathcal{S} < 0$) to stabilising ($\partial_h \mathcal{S} > 0$) close to the temperature extremes (Figure 5c,d and Figure S5.4).

The ρ–κ plane for the stability metric was split into four regions; in two regions closest to consumer extinction, $|\partial_e \mathcal{S}| = \partial_m \mathcal{S}$ were the largest sensitivities (Figure 6a, red and yellow regions) and in the two regions furthest from consumer extinction, $|\partial_K \mathcal{S}| = |\partial_a \mathcal{S}|$ ranked highest (Figure 6a, green and blue regions). Additionally, the Hopf bifurcation (Figure 6a, dashed curve) split the plane into stable equilibrium and oscillation regions. Corresponding to the general findings, stability in the two reference ('unimodal' and 'monotonic') parameterisations was most sensitive to changes in e and m at the thermal extremes—close to consumer extinction—and to a and K at milder temperatures—far from consumer extinction (Figure 6b,c). The unimodal trajectory occupied the region of oscillations for most temperatures, crossing the Hopf bifurcation twice close to consumer extinction, once at low and once at high temperatures (Figure 6b, red region). The monotonic trajectory started in the region of oscillations and moved into the stable region with warming, crossing the Hopf bifurcation far from the thermal extreme (Figure 6c, green region).

Parameter thermal dependencies alter warming–stability relationships

Plotting the other temperature parameterisations' trajectories onto the ρ–κ plane reproduced the same patterns with respect to the stability metric's sensitivity (Figure 7): stability was most sensitive to e and m at the thermal extremes and to a and K far from the extremes. Significantly, the trajectories revealed the impact of the thermal dependence shape of individual parameters on the warming–stability relationship. In three monotonic parameterisations, warming stabilised the dynamics (Figure 7a–c). In the cases, when oscillations did take place, these occurred at low temperatures (Figure 7a resident prey, b, c) and dynamics crossed the Hopf bifurcation far from the thermal boundary. In the case with two enrichment levels (Figure 7c), the high enrichment scenario required higher temperatures to stabilise the dynamics. For the unimodal trajectory with hump-shaped attack rate (Figure 7d), warming at low temperatures pushed the dynamics towards (low enrichment) or deeper into (high enrichment) the region

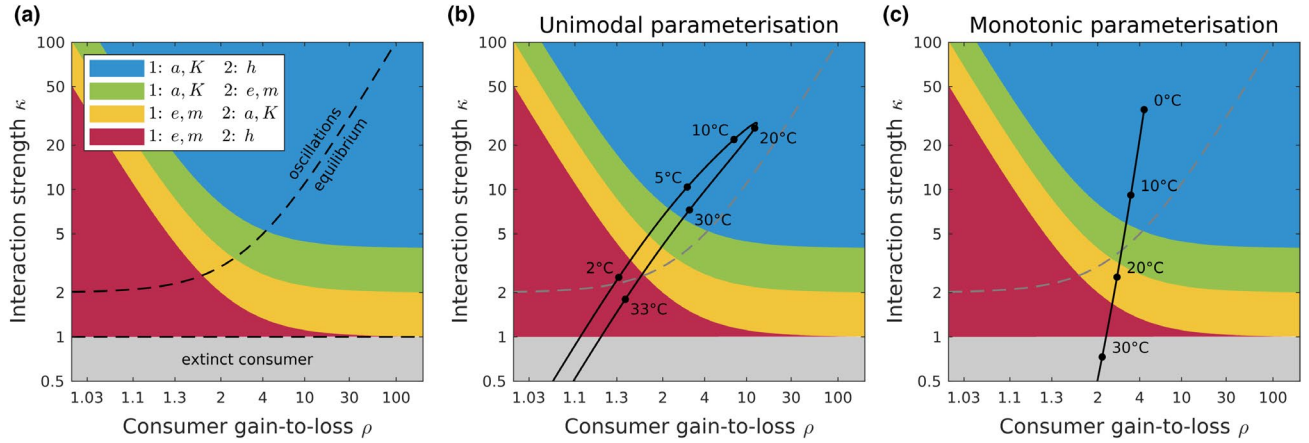


FIGURE 6 (a) Stability metric sensitivity rankings in the ρ–κ plane. The plane is split into regions (different colours) which correspond to different parameters having the top-two largest sensitivities. These regions have been derived from the analytic expressions of the elasticities (Table 1). e and m rank first close to consumer extinction; h ranks second highest closest to consumer extinction (red region). The sensitivity of stability to a and K increases moving away from consumer extinction. a and K sensitivity ranks second (yellow region), and then first moving further away. Initially, e and m rank second (green region) before h becomes significant (blue region). The plane includes the feasibility boundary ($\kappa = 1$) and the Hopf bifurcation (dotted curve splitting the plane into stable equilibrium and oscillations). For the (b) unimodal and (c) monotonic parameterisations from the literature, the thermal dependencies of $\rho = \frac{e}{mh}$ and $\kappa = \frac{K}{R_s}$ were calculated. This yielded a trajectory for each parameterisation (solid black line). The paths of the trajectories demonstrate the dynamical regime and the sensitivity of the stability metric along the temperature gradient for each parameterisation.

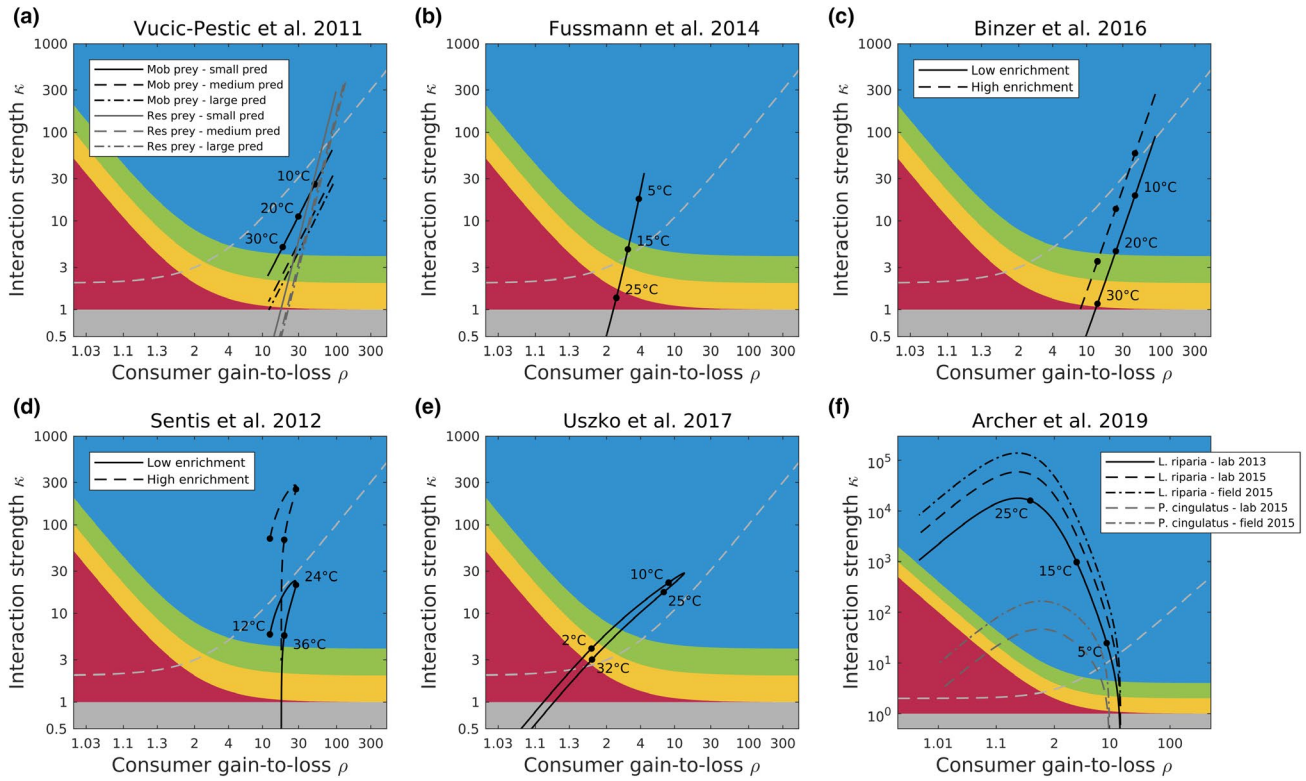


FIGURE 7 Trajectories of the six empirical temperature parameterisations in the ρ–κ plane: (a) Vucic-Pestic et al., (2011) with six different interaction experiments—three predator size classes and two types of prey, (b) Fussmann et al., (2014), (c) Binzer et al., (2016) with two levels of enrichment, (d) Sentis et al., (2012), with two levels of enrichment, (e) Uszko et al., (2017), (f) Archer et al., (2019) with two prey types and three measurements. Panels (a–c) have monotonic thermal dependences for a, m (increasing) and h, K (decreasing) and a constant e. Panel (d) has a unimodal thermal performance curve for a (hump-shaped), constant e and K, monotonic h (decreasing) and m (increasing). Panel (e) has a unimodal (U-shaped) h and a (hump-shaped) thermal dependence, constant e and monotonic K, m (increasing). Panel (f) has monotonic a, K, m, e (increasing) and h constant. All parameter values are detailed in Supporting Information S6. The coloured regions demonstrate the different biomass ratio sensitivity rankings (see legend in Figure 6a). The trajectories (solid black line) for each parameterisation are derived from calculating the thermal dependence of $\rho = \frac{e}{mh}$ and $\kappa = \frac{K}{R_S}$. Therefore, trajectories do not change with the variable of interest; the sensitivity regions do

with oscillations (i.e., destabilised dynamics). Here too, the destabilising impact of enrichment was evident. However, further warming switched the direction of the trajectory. Subsequently, both ρ and κ decreased. κ declined much faster, forcing the dynamics towards the stable region and eventually consumer extinction. Both the switch in the trajectory direction and the Hopf bifurcation (high enrichment scenario) occurred at mild temperatures, in the region of high a and K sensitivity. In the parameterisation with both a (hump-shaped) and h (U-shaped) unimodal (Figure 7e), the Hopf bifurcation occurred close to the thermal boundaries, where κ increased (low temperatures) or decreased (high temperatures) much faster than ρ. The dynamics were oscillatory for most temperatures, with the switch in the trajectory's direction occurring in the region of highest sensitivity to a and K. The final parameterisation's trajectories were characterised by a negative relationship between ρ and κ (Figure 7f). Driven by the positive thermal dependence of carrying capacity, warming increased κ and destabilised dynamics which oscillated for most temperatures.

DISCUSSION

Research on the impacts of warming on consumer–resource interactions has yielded mixed results (Englund et al., 2011; Gilbert et al., 2014; Rall et al., 2012; Uszko et al., 2017; Vasseur & McCann, 2005). Resolving this debate and improving predictions has become even more pressing as most ecosystems face increased temperatures (Easterling et al., 2000; Parmesan, 2006; Root et al., 2003; Walther et al., 2002). Here, we developed an approach to improve and simplify predictions on the impacts of warming on consumer–resource interactions. This approach integrates two pathways: (1) a sensitivity analysis to identify the key biological parameters whose variations have the largest relative impact on community properties at a given temperature and (2) aggregate parameters to increase explanatory power. We used the Rosenzweig–MacArthur model with a type II functional response and applied the approach to consumer–resource biomass ratio and a stability metric quantifying the propensity for oscillations

(Johnson & Amarasekare, 2015). Therefore, our insights and the aggregates maximal energetic efficiency, ρ, and interaction strength, κ, apply to study systems well-described by the Rosenzweig–MacArthur model. Our analyses revealed that the relative significance of different parameter groupings is determined by the proximity of the consumer to its thermal boundaries. We, further, elucidated how differences in the shape of the thermal dependence curves of individual parameters qualitatively impact predictions. We used empirically derived thermal dependence curves of biological parameters from the literature to illustrate this.

We focus our discussion on the formulation of four testable predictions arising from our results. For each prediction, we present its implications and rationale. Then, we discuss the empirical measurement of the aggregate parameters and present important subtleties and potential extensions of our approach.

Prediction 1: Resource growth rate regulates biomass distribution at mild temperatures

Implications

We showed that the relative dominance of consumer assimilation efficiency, metabolism and resource growth rate in driving changes in biomass distributions should manifest itself in any consumer–resource community far from its feasibility boundaries, assuming these communities are well-described by the Rosenzweig–MacArthur model (Figure 3a). Due to the agreement about the thermal dependence of metabolism (Fussmann et al., 2014; Rall et al., 2010; Uszko et al., 2017) and the negligible—if any—change of assimilation efficiency with warming (Dell et al., 2011), differences in the thermal performance curve of resource growth rate will strongly impact biomass ratio predictions. Therefore, improved predictions about the impacts of warming on biomass distributions at mild temperatures necessitate the accurate description of the thermal dependence of resource growth rate.

Reasoning

Far from the community thermal boundaries, consumer assimilation efficiency, metabolism and resource growth rate always had the greatest elasticity with an almost equal relative impact on biomass ratio ($\partial_e \mathcal{B} = |\partial_m \mathcal{B}| \approx \partial_r \mathcal{B} = 1$, Figure 2c,d and Figure S5.3). Increasing metabolism reduced biomass ratios (Table 1), which is likely to be a universal response across ecosystems, given the positive exponential dependence of metabolism on temperature across organisms (Brown et al., 2004; Gilooly et al., 2001; Rall et al., 2012 but see Ehnes et al., 2011). Conversely, assimilation efficiency increased biomass ratios but has either been assumed to be unaffected by temperature changes (Sentis et al., 2017; Uszko et al., 2017; Vasseur & McCann, 2005) or has yielded a weak temperature dependence (Daugaard et al., 2019; Handeland et al., 2008; Lang et al., 2017; Wurtsbaugh & Davis, 1977) with negligible change compared to other parameters. Increasing resource growth rate also increased the biomass ratio. However, evidence on the shape of resource growth's thermal response remains inconclusive: it can either increase exponentially with temperature (Savage et al., 2004) or decrease abruptly beyond the thermal optimum (Dannon et al., 2010; Thomas et al., 2012). Since the biomass ratio is directly proportional to the resource growth rate ($\partial_r \mathcal{B} = 1$, Table 1), it will be strongly affected by the values and shape of the resource growth rate thermal performance curve. Given the consensus surrounding the temperature dependence of metabolism and the minor scale of potential change in assimilation efficiency with temperature, our findings emphasise the significance of correctly parameterising the resource growth rate when aiming to predict biomass distribution changes due to warming at mild temperatures.

Prediction 2: Interaction strength determines consumer survival with increasing temperatures

Implications

If resources have a broader thermal range compared to consumers (Rose & Caron, 2007; West & Post, 2016), the thermal boundaries of the community can be determined by measuring solely the thermal dependence of interaction strength, κ. This quantity—the ratio of the resource equilibrium density without consumers (carrying capacity) to the resource equilibrium density with consumers—can be determined experimentally (Berlow et al., 2004) or through observations, facilitating predictions and cross-system comparisons thereof.

Reasoning

Close to the consumer extinction boundary, consumer survival becomes extremely sensitive to all parameters apart from resource growth (Figure 2 and Figure S5.1), making accurate predictions challenging. Currently, consumer survival has been inferred through energetic efficiency—the effective energetic gain of consumers at a certain resource density—which requires determining the thermal dependence of the functional response (Archer et al., 2019; Vucic-Pestic et al., 2011). Not only is the functional response's thermal dependence hotly contested (Uiterwaal & DeLong, 2020; Uszko et al., 2017), but this uncertainty will be exacerbated by its extremely high sensitivity at the community's thermal boundaries. We showed that there exists an alternative, empirically

more direct and theoretically more robust metric to determine consumer survival and hence community feasibility. Interaction strength—the relative values of resource equilibrium without and with consumers (Berlow et al., 1999, 2004; Gilbert et al., 2014)—provides the necessary condition for consumer survival ($\kappa > 1$), when resources are thermal generalists compared to consumers. This provides an accurate threshold and represents a measurable quantity that can be standardised across experimental designs and study systems (Berlow et al., 2004).

Prediction 3: Warming reduces community stability at low and mild temperatures

Implications

This prediction rests on important assumptions: that resources have a broader thermal range, that organisms currently experience temperatures below their optima (Pawar et al., 2016) and that the functional response is of type II with a unimodal thermal dependence (Kuiters, 2013; Rall et al., 2012; Sentis et al., 2012; Uiterwaal & DeLong, 2020; Uszko et al., 2017; West & Post, 2016). We deem these assumptions realistic based on the literature; therefore, we argue that consumer–resource interactions at low and mild temperatures will be destabilised by warming. At higher temperatures, warming should always enhance stability.

Reasoning

Stability in the context of consumer–resource interactions has predominantly referred to a qualitative distinction between stable and oscillating dynamics (Rosenzweig & MacArthur, 1963; Vasseur & McCann, 2005; Yodzis & Innes, 1992). We based our analysis on an adjusted stability metric which quantifies the tendency of dynamics to oscillate (Johnson & Amarasekare, 2015, Supporting Information S4). When comparing existing temperature parameterisations, we found that in most monotonic parameterisations (increasing metabolism and attack rate, decreasing handling time and carrying capacity and assimilation efficiency constant), warming always (i.e., monotonically) stabilised dynamics (Figure 7a–c). The single exception arose when temperature and carrying capacity increased simultaneously, which destabilised dynamics (Figure 7f). Carrying capacity has been described as a proxy for enrichment, and its destabilising effect has been established whether independently of temperature (Rosenzweig, 1971) or as antagonistic to warming (Binzer et al., 2016). When at least one parameter in the functional response had a unimodal thermal dependence (i.e., hump-shaped attack rate or U-shaped handling time), this yielded a unimodal warming–stability relationship (Figure 7d,e). Significantly, the divergence between the unimodal and (most) monotonic parameterisations in the predicted effect of warming on stability manifested itself at low or mild, rather than high temperatures (Figures 6 and 7). This pattern originates in the impact of the parameters with unimodal thermal dependencies on stability. Attack rate is destabilising (Table 1, McCann, 2011). Thus, a hump-shaped thermal dependence of attack rate destabilises dynamics with warming below the thermal optimum and stabilises dynamics beyond it. Increases in handling time are stabilising close to the thermal extremes (Figure 6c and Figure S5.2). A U-shaped handling time will rapidly decrease with warming from low temperatures, which is strongly destabilising; a corresponding steep increase at high temperatures produces a strong stabilising effect. Thus, warming at high temperatures will always be stabilising. However, at lower temperatures, unimodal and monotonic thermal dependencies produce contrasting warming–stability relationships. Therefore, the thermal dependence shape of the functional response combined with the temperatures currently experienced by communities relative to their optimal temperature will determine the impact of warming on stability (Betini et al., 2019).

Prediction 4: Warming stabilises dynamics only when interaction strength decreases faster than maximal energetic efficiency

Implications

The combination of ρ—the energetic gain-to-loss ratio of consumers given unlimited resources—and κ—interaction strength—accurately describes the warming–stability relationship with no recourse to the thermal dependence shapes of individual parameters, the current temperatures relative to the thermal optima or the proximity to the thermal boundaries of the community. Therefore, differential responses of resources and consumers to warming (Dell et al., 2014) will be encompassed by the thermal dependence of the aggregates—assuming the consumer–resource system is well-described by the Rosenzweig–MacArthur model. The Hopf bifurcation condition (Equation 6) dictates that κ should decrease faster than ρ for warming to stabilise consumer–resource interactions. Thus, measuring ρ and κ directly can increase the accuracy of warming–stability predictions and simplify cross-system comparisons.

Reasoning

Decreasing energetic efficiency or interaction strength has been considered equivalent to increasing stability (Rall et al., 2008, 2010; Sentis et al., 2012). Thus, estimates of consumer energetic efficiency or interaction

strength based on empirically derived thermal dependence curves of individual rates (e.g., ingestion rate, attack rate and metabolic rate) have been used to infer the impacts of warming on stability (Fussmann et al., 2014; Rall et al., 2010, 2012; Vucic-Pestic et al., 2011). However, this raises two significant issues. On the one hand, even subtle changes in the thermal dependence shapes of individual parameters can yield all possible outcomes (Amarasekare, 2015). On the other hand, reducing the analysis of stability to a single aggregate parameter has limitations. Gilbert et al., (2014) described the warming–stability relationship with a single aggregate, interaction strength, but their approach was based on a type I functional response and its predictions do not work well in type II or III scenarios (Uszko et al., 2017). Johnson and Amarasekare (2015) and Amarasekare (2015) attained a single aggregate parameter to reduce the complexity of their explorations; however, this lacks descriptive power of the dynamics close to the community's thermal boundaries (Supporting Information S4). Our analysis in the ρ–κ plane suggests that stability cannot be reduced to a single aggregate parameter nor does a decrease in either one or both of ρ and κ suffice to stabilise dynamics. In fact, both ρ and κ can decrease with warming while dynamics become destabilised. A stabilising effect of warming requires not only a concurrent reduction in ρ and κ but also the latter to decrease faster. Critically, both ρ and κ represent biological quantities which can be consistently measured across study systems.

Working with aggregate parameters

Working directly with the two aggregate parameters, maximal consumer energetic efficiency, ρ, and interaction strength, κ, can simplify empirical measurements and improve the accuracy of theoretical predictions, particularly for field data and experiments, as we argue below. To determine the thermal dependence of maximal consumer energetic efficiency and interaction strength, one can measure consumer population growth given unlimited resources and resource population density in the presence and absence of consumers at different temperatures, respectively. Interaction strength is commonly determined in field experiments where consumers are excluded (Berlow et al., 2004; Estes et al., 2011; Novak, 2010; Wootton & Emmerson, 2005). Consumer energetic gain-to-loss ratio under effectively unlimited resources is more rarely estimated. However, it can be derived from consumer population net growth and metabolism and mortality, quantities measured commonly in the field and in the lab (Hanson & Peters, 1984; Lampert et al., 1986; Stemberger & Gilbert, 1985). Moreover, confounding factors in field measurements of the population-level aggregates should generate less uncertainty compared to that of measuring multiple individual parameters, where uncertainty propagates and often generates large uncertainty in model predictions (e.g., Sentis et al., 2015). Therefore, working directly with aggregate parameters can be both simpler and lead to more accurate predictions in the field. On the other hand, measuring individual parameters in the lab has well-established protocols and a history of reliable outputs, with measurements requiring only short-term experiments as opposed to the aggregates.

The choice between measuring aggregate or individual parameters will be informed by the questions and objectives of each study. The aggregates describe population-level mechanisms of consumer–resource interactions, while individual parameters correspond to physiological or behavioural processes of individual organisms scaled up to the population level. As we argued, aggregates can provide more accurate predictions for field measurements whereas individual parameters can be accurately measured in the lab. This does raise the question whether measurements in a controlled laboratory environment can represent noisier field conditions. It would be useful to compare directly measured aggregate parameters to aggregate parameter values derived from individual parameters to determine how well predictions based on individual rates capture the dynamics of the system. Regardless of the choice, our approach provides the tools for both pathways: studies working with individual parameters will benefit from identifying the most important parameters to measure, while aggregate parameter data points can be directly mapped onto the ρ–κ landscape.

Subtleties and extensions

The sensitivity analysis quantified the sensitivity of the model variables to small parameter changes. Therefore, applying its insights to data should take into consideration the scales of parameters in the temperature range of interest and potential uncertainties in the parameter estimates (Manlik et al., 2018). Hence, our argument for the reduced significance of the thermal dependence of assimilation efficiency in driving changes in biomass distributions, despite its high sensitivity.

Regarding the stability of consumer–resource interactions, the ρ–κ plane helped visualise the stabilising effect of a type III functional response (Figure S2.1), which has both theoretical and empirical support (Daugaard et al., 2019; Kalinkat et al., 2013; Sarnelle & Wilson, 2008; Uszko et al., 2017). For the type II response, the defining role of the functional response (attack rate) and the carrying capacity has been widely documented (Amarasekare, 2015; Binzer et al., 2016; Johnson & Amarasekare, 2015; Rosenzweig, 1971); we add the important caveat that this is the case only far from consumer extinction (Figure 6a).

Finally, relaxing certain assumptions can extend our approach. Considering the scenario where the consumer has a broader thermal niche relative to that of the resource

will make the thermal limits of coexistence dependent on resource growth (Amarasekare, 2015). Considering the extinction of populations with very low abundances to account for stochastic extinctions can define a realisable coexistence range within the feasible parameter space. Breaking down the original model parameters (e.g., handling time includes the handling and ingestion of prey) could facilitate our understanding of the role of more fundamental physiological processes in the dynamics. Finally, climate change will lead to stronger fluctuations in temperatures (IPCC, 2013), which have been shown to alter predictions in consumer–resource dynamics (Dee et al., 2020; Vasseur et al., 2014). This makes the inclusion of temperature variability an important next step.

CONCLUSIONS

Warming will have significant but as yet uncertain impacts on consumer–resource interactions which underpin the structure and functioning of ecosystems. We presented an approach that will help to improve the accuracy of predictions and reconcile divergent results by facilitating cross-system comparisons. This approach first determines the parameters whose variations have the largest effect on community properties. Second, it simplifies analyses to a two-dimensional plane of mechanistically tractable aggregate parameters. Applying it to the Rosenzweig–MacArthur model, we showed that close to the consumer extinction boundary (i.e., at temperature extremes) both consumer–resource biomass ratio and stability are most sensitive to changes in consumer assimilation efficiency and metabolism. Far from the boundary (i.e., mild temperatures), biomass ratio is most sensitive to resource growth rate, consumer assimilation efficiency and metabolism. This yielded our first prediction that resource growth rate regulates biomass distributions at mild temperatures. The consensus around the thermal dependence of metabolism and the limited potential impact of warming on assimilation efficiency underscore the importance of correctly measuring the thermal dependence of resource growth rate. Using the two aggregate parameters (interaction strength and consumer maximal energetic efficiency) also simplified the study of important properties of consumer–resource interactions. From this followed our second prediction that the thermal boundaries of the community are defined by interaction strength alone. In terms of stability, we demonstrated that a unimodal thermal dependence of attack rate or handling time alters predictions of warming–stability relationships below the thermal optimum, where many organisms may be currently living. Hence, our third prediction is that initial increases in mean temperatures will destabilise consumer–resource interactions. Significantly, our approach elucidates how the thermal dependence of stability can be comprehensively characterised by maximal energetic efficiency and interaction strength values. This produced our fourth prediction: a faster reduction of interaction strength than of maximal energetic efficiency with warming is necessary for dynamics to stabilise. Finally, we demonstrated the potential for targeted experiments to measure the thermal dependencies of maximal energetic efficiency and interaction strength to improve predictions. Ultimately, we show that any temperature parameterisation fitted to the Rosenzweig–MacArthur model can be mapped onto the aggregate parameter plane, revealing its stability landscape, providing a mechanistic interpretation for its predictions and allowing for the cross-system comparison of these predictions.

ACKNOWLEDGEMENTS

We thank three anonymous reviewers, Ulrich Brose and John Drake for their constructive feedback. This research is supported by the FRAGCLIM Consolidator Grant, funded by the European Research Council under the European Union's Horizon 2020 research and innovation programme (Grant Agreement Number 726176) and by the 'Laboratoires d'Excellences (LABEX)' TULIP (ANR-10-LABX-41).

CONFLICT OF INTEREST

The authors declare no competing interests.

AUTHOR CONTRIBUTIONS

ADS, BH, AS and JMM conceived the approach. ADS and BH developed the method, AS and JMM guided its application. ADS led the writing of the manuscript; BH, AS and JMM provided crucial input and guidance throughout the writing process. JMM obtained the funding and managed the project.

PEER REVIEW

The peer review history for this article is available at https://publons.com/publon/10.1111/ele.13780.

DATA AVAILABILITY STATEMENT

This study produced no new data. Any data used were taken from existing publication and are detailed in the supporting information.

ORCID

Alexis D. Synodinos https://orcid.org/0000-0001-9646-2688
Bart Haegeman https://orcid.org/0000-0003-2325-4727
Arnaud Sentis https://orcid.org/0000-0003-4617-3620
José M. Montoya https://orcid.org/0000-0002-6676-7592

REFERENCES

Amarasekare, P. (2015) Effects of temperature on consumer-resource interactions. *Journal of Animal Ecology*, 84, 665–679.

Amarasekare, P. (2019) Effects of climate warming on consumer-resource interactions: a latitudinal perspective. *Frontiers in Ecology and Evolution*, 7, 146.

Archer, L.C., Sohlström, E.H., Gallo, B., Jochum, M., Woodward, G., Kordas, R.L. et al. (2019) Consistent temperature dependence of functional response parameters and their use in predicting population abundance. *Journal of Animal Ecology*, 88, 1670–1683.

Barbier, M. & Loreau, M. (2019) Pyramids and cascades: a synthesis of food chain functioning and stability. *Ecology Letters*, 22, 405–419.

Berlow, E.L., Navarrete, S.A., Briggs, C.J., Power, M.E. & Menge, B.A. (1999) Quantifying variation in the strengths of species interactions. *Ecology*, 80, 2206.

Berlow, E.L., Neutel, A.-M., Cohen, J.E., de Ruiter, P.C., Ebenman, B.O., Emmerson, M. et al. (2004) Interaction strengths in food webs: issues and opportunities. *Journal of Animal Ecology*, 73(3), 585–598.

Betini, G.S., Avgar, T., McCann, K.S. & Fryxell, J.M. (2019) Temperature triggers a non-linear response in resource–consumer interaction strength. *Ecosphere*, 10(8), e02787. https://doi.org/10.1002/ecs2.2787

Bideault, A., Galiana, N., Zelnik, Y.R., Gravel, D., Loreau, M., Barbier, M. et al. (2020) Thermal mismatches in biological rates determine trophic control and biomass distribution under warming. *Global Change Biology*, 27(2), 257–269.

Binzer, A., Guill, C., Brose, U. & Rall, B.C. (2012) The dynamics of food chains under climate change and nutrient enrichment. *Philosophical Transactions of the Royal Society B: Biological Sciences*, 367, 2935–2944.

Binzer, A., Guill, C., Rall, B.C. & Brose, U. (2016) Interactive effects of warming, eutrophication and size structure: impacts on biodiversity and food-web structure. *Global Change Biology*, 22, 220–227.

Brown, J.H., Gillooly, J.F., Allen, A.P., Savage, V.M. & West, G.B. (2004) Toward a metabolic theory of ecology. *Ecology*, 85, 1771–1789.

Caswell, H. (2019) *Sensitivity analysis: matrix methods in demography and ecology*. Demographic research monographs. Cham, Switzerland: Springer International Publishing.

Chitnis, N., Hyman, J.M. & Cushing, J.M. (2008) Determining important parameters in the spread of malaria through the sensitivity analysis of a mathematical model. *Bulletin of Mathematical Biology*, 70, 1272–1296.

Dannon, E.A., Tamò, M., van Huis, A. & Dicke, M. (2010) Functional response and life history parameters of *Apanteles taragamae*, a larval parasitoid of *Maruca vitrata*. *BioControl*, 55, 363–378.

Daugaard, U., Petchey, O.L. & Pennekamp, F. (2019) Warming can destabilize predator–prey interactions by shifting the functional response from Type III to Type II. *Journal of Animal Ecology*, 88, 1575–1586.

Dee, L.E., Okamtoto, D., Gårdmark, A., Montoya, J.M. & Miller, S.J. (2020) Temperature variability alters the stability and thresholds for collapse of interacting species. *Philosophical Transactions of the Royal Society B: Biological Sciences*, 375, 20190457.

Dell, A.I., Pawar, S. & Savage, V.M. (2011) Systematic variation in the temperature dependence of physiological and ecological traits. *Proceedings of the National Academy of Sciences of the United States of America*, 108, 10591–10596.

Dell, A.I., Pawar, S. & Savage, V.M. (2014) Temperature dependence of trophic interactions are driven by asymmetry of species responses and foraging strategy. *Journal of Animal Ecology*, 83, 70–84.

Deutsch, C.A., Tewksbury, J.J., Huey, R.B., Sheldon, K.S., Ghalambor, C.K., Haak, D.C. et al. (2008) Impacts of climate warming on terrestrial ectotherms across latitude. *Proceedings of the National Academy of Sciences of the United States of America*, 105, 6668–6672.

Easterling, D.R., Meehl, G.A., Parmesan, C., Changnon, S.A., Karl, T.R. & Mearns, L.O. (2000) Climate extremes: observations, modeling, and impacts. *Science*, 289, 2068–2074.

Ehnes, R.B., Rall, B.C. & Brose, U. (2011) Phylogenetic grouping, curvature and metabolic scaling in terrestrial invertebrates. *Ecology Letters*, 14, 993–1000.

Englund, G., Öhlund, G., Hein, C.L. & Diehl, S. (2011) Temperature dependence of the functional response. *Ecology Letters*, 14, 914–921.

Estes, J.A., Terborgh, J., Brashares, J.S., Power, M.E., Berger, J., Bond, W.J. et al. (2011) Trophic downgrading of planet earth. *Science*, 333, 301–306.

Fussmann, K.E., Schwarzmüller, F., Brose, U., Jousset, A. & Rall, B.C. (2014) Ecological stability in response to warming. *Nature Climate Change*, 4, 206–210.

Gilbert, B., Tunney, T.D., McCann, K.S., DeLong, J.P., Vasseur, D.A., Savage, V. et al. (2014) A bioenergetic framework for the temperature dependence of trophic interactions. *Ecology Letters*, 17, 902–914.

Gillooly, J.F., Brown, J.H., Geoffrey, B.W., Savage, V.M. & Charnov, E.L. (2001) Effects of size and temperature on metabolic rate. *Science*, 293, 2248–2251.

Handeland, S.O., Imsland, A.K. & Stefansson, S.O. (2008) The effect of temperature and fish size on growth, feed intake, food conversion efficiency and stomach evacuation rate of Atlantic salmon post-smolts. *Aquaculture*, 283, 36–42.

Hanson, J.M. & Peters, R.H. (1984) Empirical prediction of crustacean zooplankton biomass and profundal macrobenthos biomass in lakes. *Canadian Journal of Fisheries and Aquatic Sciences*, 41, 439–445.

IPCC. (2013) *Climate change 2013: the physical science basis. Contribution of working group I to the fifth assessment report of the intergovernmental panel on climate change*. In: Stocker, T.F., Qin, D., Plattner, G.-K., Tignor, M., Allen, S.K. & Boschung, J. (Eds.). Cambridge, UK; New York, NY: Cambridge University Press.

Jeschke, J.M., Kopp, M. & Tollrian, R. (2004) Consumer-food systems: why type I functional responses are exclusive to filter feeders. *Biological Reviews*, 79(2), 337–349.

Johnson, C.A. & Amarasekare, P. (2015) A metric for quantifying the oscillatory tendency of consumer-resource interactions. *The American Naturalist*, 185, 87–99.

Kalinkat, G., Schneider, F.D., Digel, C., Guill, C., Rall, B.C. & Brose, U. (2013) Body masses, functional responses and predator-prey stability. *Ecology Letters*, 16, 1126–1134.

Kuiters, A.T. (2013) Diversity–stability relationships in plant communities of contrasting habitats. *Journal of Vegetation Science*, 24, 453–462.

Lampert, W., Fleckner, W., Rai, H. & Taylor, B.E. (1986) Phytoplankton control by grazing zooplankton: a study on the spring clear-water phase. *Limnology and Oceanography*, 31, 478–490.

Lang, B., Ehnes, R.B., Brose, U. & Rall, B.C. (2017) Temperature and consumer type dependencies of energy flows in natural communities. *Oikos*, 126, 1717–1725.

Manlik, O., Lacy, R.C. & Sherwin, W.B. (2018) Applicability and limitations of sensitivity analyses for wildlife management. *Jouranl of Applied Ecology*, 55, 1430–1440.

May, R.M. (1972) Limit cycles in predator-prey communities. *Science*, 177, 900–902.

McCann, K.S. (2011) *Food webs (MPB-50)*. Princeton University Press. Monograph Pop Bio. Available at: https://press.princeton.edu/books/paperback/9780691134185/food-webs-mpb-50 [Accessed 10 September 2020].

Montoya, J.M. & Raffaelli, D. (2010) Climate change, biotic interactions and ecosystem services. *Philosophical Transactions of the Royal Society B: Biological Sciences*, 365, 2013–2018.

Novak, M. (2010) Estimating interaction strengths in nature: experimental support for an observational approach. *Ecology*, 91, 2394–2405.
O'Connor, M.I., Piehler, M.F., Leech, D.M., Anton, A. & Bruno, J.F. (2009) Warming and resource availability shift food web structure and metabolism. *PLoS Biology*, 7, e1000178.
Parmesan, C. (2006) Ecological and evolutionary responses to recent climate change. *Annual Review of Ecology, Evolution, and Systematics*, 37, 637–669.
Pawar, S., Dell, A.I., Savage, V.M. & Knies, J.L. (2016) Real versus artificial variation in the thermal sensitivity of biological traits. *The American Naturalist*, 187, E41–E52.
Petchey, O.L., Brose, U. & Rall, B.C. (2010) Predicting the effects of temperature on food web connectance. *Philosophical Transactions of the Royal Society B: Biological Sciences*, 365, 2081–2091.
Pörtner, H.O. & Farrell, A.P. (2008) Ecology: physiology and climate change. *Science*, 322(5902), 690–692.
Rall, B.C., Brose, U., Hartvig, M., Kalinkat, G., Schwarzmüller, F., Vucic-Pestic, O. et al. (2012) Universal temperature and body-mass scaling of feeding rates. *Philosophical Transactions of the Royal Society B: Biological Sciences*, 367, 2923–2934.
Rall, B., Guill, C. & Brose, U. (2008) Food-web connectance and predator interference dampen the paradox of enrichment. *Oikos*, 117, 202–213.
Rall, B.Ö.C., Vucic-Pestic, O., Ehnes, R.B., EmmersoN, M. & Brose, U. (2010) Temperature, predator-prey interaction strength and population stability. *Global Change Biology*, 16, 2145–2157.
Réveillon, T., Rota, T., Chauvet, É., Lecerf, A. & Sentis, A. (2019) Repeatable inter-individual variation in the thermal sensitivity of metabolic rate. *Oikos*, 128, 1633–1640.
Rip, J.M.K. & McCann, K.S. (2011) Cross-ecosystem differences in stability and the principle of energy flux. *Ecology Letters*, 14, 733–740.
Root, T.L., Price, J.T., Hall, K.R., Schneider, S.H., Rosenzweig, C. & Pounds, J.A. (2003) Fingerprints of global warming on wild animals and plants. *Nature*, 421, 57–60.
Rose, J.M. & Caron, D.A. (2007) Does low temperature constrain the growth rates of heterotrophic protists? Evidence and implications for algal blooms in cold waters. *Limnology and Oceanography*, 52, 886–895.
Rosenzweig, M.L. (1971) Paradox of enrichment: destabilization of exploitation ecosystems in ecological time. *Science*, 171, 385–387.
Rosenzweig, M.L. & MacArthur, R.H. (1963) Graphical representation and stability conditions of predator-prey interactions. *The American Naturalist*, 97, 209–223.
Sarnelle, O. & Wilson, A.E. (2008) Type III functional response in *Daphnia*. *Ecology*, 89, 1723–1732.
Savage, V.M., Gilloly, J.F., Brown, J.H., Charnov, E.L. & Charnov, E.L. (2004) Effects of body size and temperature on population growth. *The American Naturalist*, 163, 429–441.
Sentis, A., Binzer, A. & Boukal, D.S. (2017) Temperature-size responses alter food chain persistence across environmental gradients. *Ecology Letters*, 20, 852–862.
Sentis, A., Hemptinne, J.L. & Brodeur, J. (2012) Using functional response modeling to investigate the effect of temperature on predator feeding rate and energetic efficiency. *Oecologia*, 169, 1117–1125.
Sentis, A., Morisson, J. & Boukal, D.S. (2015) Thermal acclimation modulates the impacts of temperature and enrichment on trophic interaction strengths and population dynamics. *Global Change Biology*, 21, 3290–3298.
Stemberger, R.S. & Gilbert, J.J. (1985) Body size, food concentration, and population growth in planktonic rotifers. *Ecology*, 66, 1151–1159.
Thakur, M.P., Künne, T., Griffin, J.N. & Eisenhauer, N. (2017) Warming magnifies predation and reduces prey coexistence in a model litter arthropod system. *Proceedings of the Royal Society B: Biological Sciences*, 284, 20162570.
Thomas, M.K., Kremer, C.T., Klausmeier, C.A. & Litchman, E. (2012) A global pattern of thermal adaptation in marine phytoplankton. *Science*, 338, 1085–1088.
Uiterwaal, S.F. & DeLong, J.P. (2020) Functional responses are maximized at intermediate temperatures. *Ecology*, 101(4), e02975. https://doi.org/10.1002/ecy.2975
Uszko, W., Diehl, S., Englund, G. & Amarasekare, P. (2017) Effects of warming on predator-prey interactions – A resource-based approach and a theoretical synthesis. *Ecology Letters*, 20, 513–523.
Vasseur, D.A., DeLong, J.P., Gilbert, B., Greig, H.S., Harley, C.D.G., McCann, K.S. et al. (2014) Increased temperature variation poses a greater risk to species than climate warming. *Proceedings of the Royal Society B: Biological Sciences*, 281(1779), 20132612.
Vasseur, D.A. & McCann, K.S. (2005) A mechanistic approach for modeling temperature-dependent consumer-resource dynamics. *The American Naturalist*, 166, 184–198.
Vucic-Pestic, O., Ehnes, R.B., Rall, B.C. & Brose, U. (2011) Warming up the system: higher predator feeding rates but lower energetic efficiencies. *Global Change Biology*, 17, 1301–1310.
Walther, G.-R., Post, E., Convey, P., Menzel, A., Parmesan, C., Beebee, T.J.C. et al. (2002) Ecological responses to recent climate change. *Nature*, 416, 389–395.
West, D.C. & Post, D.M. (2016) Impacts of warming revealed by linking resource growth rates with consumer functional responses. *Journal of. Animal Ecology*, 85, 671–680.
Wootton, J.T. & Emmerson, M. (2005) Measurement of interaction strength in nature. *Annual Reviews in Ecology Evolution and Systematics*, 36, 419–444.
Wurtsbaugh, W.A. & Davis, G.E. (1977) Effects of temperature and ration level on the growth and food conversion efficiency of *Salmo gairdneri*, Richardson. *Journal of Fish Biology*, 11, 87–98.
Yodzis, P. & Innes, S. (1992) Body size and consumer-resource dynamics. *The American Naturalist*, 139, 1151–1175.
Zhang, L., Takahashi, D., Hartvig, M. & Andersen, K.H. (2017) Food-web dynamics under climate change. *Proceedings of the Royal Society B: Biological Sciences*, 284, 20171772.
Zhao, Q., Liu, S. & Niu, X. (2020) Effect of water temperature on the dynamic behavior of phytoplankton–zooplankton model. *Applied Mathematics and Computation*, 378, 125211.

SUPPORTING INFORMATION

Additional supporting information may be found online in the Supporting Information section.

How to cite this article: Synodinos AD, Haegeman B, Sentis A, Montoya JM. Theory of temperature-dependent consumer-resource interactions. *Ecology Letters*, 2021;24:1539–1555. https://doi.org/10.1111/ele.13780